Supplementary Materials

Site descriptions

Site maps, photographs and more detailed site descriptions can be found in Von Voigtlander (2016).

Road Cut (east and west) Road Cut sites are along Highway 270. The east site was located directly above the section interpreted by Goodfellow et al., (2013), and the Road Cut west site is located across Highway 270 from the east site. Both locations host sparse vegetation including small trees and grasses and have a MAP of 500 m/yr (Giambelluca et al., 2013). Two P-wave lines were run with 3 and 1 meter spacing on top of a 4.2 m tall road cut at an elevation of 78 m above sea level. One P-wave line with 3 meter spacing was run on the Road Cut West site on top of a 3 m high at the road cut. One S-wave line was run with 1 meter spacing on the east site. The S-wave lines, and the P-wave lines, share a centerline. The S-wave line was translated by one sensor spacing (1 m) in the array direction six times for developing the 2D S-wave profile. This resulted in a total survey line length of 21. A source offset distance of 3 m was used.

Sapphire Cove The Sapphire Cove lies 3.2 km north of the Road Cut location at an elevation of 8 m, 30 m from the shoreline and receives 500 mm/yr MAP (Giambelluca et al., 2013). Two P-wave surveys were performed here with 1 m (line 1) and 2.5 m (line 2). The survey line 2 was run parallel to the ocean and perpendicular to line 1. Like the Road Cut site, core stones were visible at the ground surface and were interspersed with soil that hosts sparse grasses and a few trees.

Kapa'a Beach Kapa'a Beach is located 4.5 km north of Sapphire Cove and 30 m from the shoreline at an elevation of 2 m above sea level. Vegetation consists of Koa trees and grass; the MAP is 604 mm/yr (Giambelluca et al., 2013). One P-wave line with 1.5 meter spacing was run perpendicular to the shoreline.

Airport The Airport site is located west of the Upolu Airport, at the northern tip of the Kohala peninsula about 7.8 km north of Kapa'a Beach and at 8 m above sea level. This site is in the transition from relatively dry to wet sites, with an MAP of 1000 mm/yr (Giambelluca et al., 2013). The vegetation consists of grasses and no trees are present near the survey lines. Three parallel and overlapping P-wave lines were run on a grassy hill about 30 meters back from a sea cliff. Lines 1 and 2 had geophone spacing of 3 m with six overlapping geophones totaling a length of 72 m. Line 3 had geophone spacing of 1 m, a total length of 15 m and was run parallel along the centerline of lines 1 and 2 (3 m spacing). One S-wave line was run with 1 m spacing. The survey line was positioned with the same centerline as P-wave lines 1 and 2, and 3. S-wave line was translated by one sensor spacing twelve times for line 2 for developing the 2D S-wave profile. This resulted in total survey line length of 27 m. A source offset distance of 3 m was used.

Lighthouse The lighthouse site is located at the Kauhola Point lighthouse, about 10 km to the southeast of the Airport site (MAP 1510 mm/yr, Giambelluca et al., 2013). Three parallel and overlapping P wave arrays were run and positioned 10 m back from the edge of the sea cliff, which is approximately 7 m above sea level. Surveys were run on a grassy area adjacent to a grove of trees. Surveys 1 and 2 were recorded with six overlapping geophones spaced 2 m apart with a total array length of 52 m. Line 3 had 3 m spacing with an array length of 45. The active erosion of the sea cliff provides fresh exposure of the subsurface profile along the vertical cliff faces. One S-wave survey line was run at this site with a spacing of 2 m. The centerline of the survey line was positioned equidistant between the centerlines of P-wave lines 1 and 2. The S-wave line was translated by one sensor spacing twelve times for a total survey line length of 54 m. A source offset of 5 m was used for S-wave line shots.

Awini Landslide The Awini site is located along the re-established Awini trail, which traverses the amphitheater canyons on the wet side of the island. This trail was demolished during landsliding caused by the 2006 M_w6.7 Kiholo Bay earthquake (Harp et al., 2012). The re-established trail crosses a large landslide just below the base of its headscarp along a steep (~ 40 degree) slope. This site receives 2070 mm/yr MAP (Giambelluca et al., 2013). The vegetation at this site had been mostly stripped away by rock fall during and since the earthquake except for the presence of grasses. One P-wave line was collected along a narrow footpath parallel to the slope using geophones spaced 1 m apart.

Waipio Canyon The Waipio Canyon site (1169 m asl) is located on the wet side of the Kohala peninsula at the head of one of the deeply incised “amphitheater canyons” (e.g. Lamb et al., 2007). This site is 23 km south of the Lighthouse site and has the highest MAP of all our study sites (3060 mm/yr) (Giambelluca et al., 2013). One P-wave survey was collected with 3 m geophone spacing. The array was run on a dirt road with slightly compacted soil surrounded by dense vegetation.

Shot locations at the west end of the array (position 45 m) produced audible vibrations and sensible ground shaking when the plate was struck, but the east end of the array did not produce these same observations. We speculate that a large void was present at depth on the west end of the line; however, we are not able to resolve a low-velocity layer using the applied methods. We note that the RMSE of the inferred models are much higher at this site compared to our other surveys. The presence of a void beneath the west end of the array may explain the thicker layer lower velocities on that end of the profile.

P-wave data and modeling P-wave models were derived by a refraction method using the first-arrivals of seismic energy, collected by a reciprocal survey (shots are conducted at either end and within the profile). Details of modeling parameters tested for each site are further elaborated in Von Voigtlander (2016). Using the Seisimager software module “Pickwin” (OYO Corporation, 2006; Hayashi and Takahashi (2011)), the waveform data from each line was displayed and first-break picks (FPB) were first automatically assigned then manually adjusted.Following waveform interpretation, FBPs were imported into the Seisimager analysis platform, “Plotrefa” (OYO Corporation, 2006), and displayed as travel-time curves. Plotrefa was used to analyze variations in the travel-time curves and invert for the velocity structure of the shallow subsurface. Prior to interpretation, the travel-time curves were checked for reciprocity in order to ensure data quality. The Principle of Reciprocity states that velocity is independent of direction of travel, meaning that the rate of wave propagation from the source to the receiver should be equal to the rate if the direction was reversed and traveled from the receiver to the source, regardless of subsurface anomalies (e.g. Hayashi and Takahashi, 2011). FBPs were corrected if the error was larger than 5%, resulting in a velocity model with smaller residuals. The travel-time curves were then inverted using Plotrefa to produce a 2D velocity model using a linearized tomographic inversion. Examples from a dry and wet sites are shown in Supplementary Figures 1 and 2. For dry sites, the uneven soil coverage and patchy exposure of core stones resulted in a more complicated near surface travel time curve compared to wet sites that had a well developed soil profile in the upper few meters.

A linearized tomographic inversion is suitable for sites with complicated velocity structures and lateral velocity variations, and can be applied to areas of both less distinct velocity contrasts as well as a layered subsurface with sharp velocity contrasts. Prior to inversion, an initial model must be constructed using a velocity range and assigning the number of layers in the model. A sensitivity analysis was performed to quantify dependence of the final velocity cross-sections on the initial model using line 1 taken from the Airport site (Supplementary Figure 3). Fifty independent linear initial velocity models were constructed; minimum velocities fell between 50-250 mm/s whereas maximum velocities ranged from 3000-5000 m/s at 20 km depth. We invert data from the Lighthouse site for each of these initial velocity profiles and calculate the average velocity and standard deviation of velocity across the profile. The average standard deviation of velocities within the profile was 40 m/s, and the maximum standard deviation is 0.13 km/s within the upper 2 m of the survey. From these results, we suggest that the choice of the initial model does not influence the final velocity model at the resolution of our interpretation, in which we evaluate different weathering layers with hundreds of m/s velocity difference.

For our final inversions, we computed the linearized tomographic inversion by iteratively tracing rays through nodes bounded by velocity cells, and therefore constructing the fastest theoretical travel times for an individual ray path. The difference between the observed and theoretical travel times for the ray paths was given by the RMSE and allows assessment of the validity of the inferred velocity models. We assigned velocity layers to the linearized tomographic inversion to aid in visual interpretation of the data.

Three 1-D Vp profiles were collected at a site of a historic flow (1859 AD) near Kiholo Bay (south of Kohala) in order to evaluate the velocity of fresh, chemically unaltered pahohoe basalt in this environment. The results of these profiles suggest near surface velocities of ~ 300 – 1000 m/s, which are substantially lower than “typical” basalt velocities (> 5000 m/s; Barton, 2007) and likely reflect initial fracturing and porosity in fresh lava flows.

MASW data and modeling All modeling was performed in the SeisImager SW/2D software suite (OYO Corporation, 2006). Two-dimensional and one-dimensional

S-wave profiles were modeled using different methods. For one-dimensional S-wave profiling, the Park et al. (1998) method was used to develop the frequency-velocity spectrum. Dispersion curve points were selected by manually picking spectral peaks in the frequency-velocity domain. For two-dimensional S-wave profiling, the Hayashi and Suzuki (2004) common-midpoint cross-correlation (CMPCC) method was used to develop the frequency-velocity spectra. The dispersion curves were similarly picked by selecting spectral peaks in each respective spectrum of the 2D array. The surface wave dispersion curves were compared to the dispersion curves of initially assumed S-wave profiles with consideration for higher mode Rayleigh waves (Xia et al., 2003). The S-wave profiles were manually adjusted and the dispersion curves recalculated until the best fit with surface wave dispersion curves was achieved. This is often routinely done by determining a nonlinear-least-squares solution. Manual adjustments are made to the S-wave model to ensure the dispersion curves match closely across all frequencies. Lower frequency Rayleigh waves induce particle motion at greater depths in the subsurface (Stokoe and Santamarina, 2000). Therefore it is important to have close matching across all frequencies in order to have a reliable S-wave model. S-wave modeling and dispersion curve matching was performed in the WaveEQ module of the Seisimager SW/2D software suite. When the closest dispersion curve match is achieved, the S-wave profile for the modeled dispersion curve is taken as the 1D final profile. For a 2D MASW survey, this is done for each CMPCC dispersion curve. The individual 1D profiles are then compiled into a 2D cross-section profile. The incorporation of individual S-wave profile sections into a complete 2D profile was performed in the GeoPlot module of the SeisImager SW/2D software suite. Example plots of 2D survey design, frequency-phase velocity diagrams, and dispersion curves are shown for each site (Supplementary Materials Figures 5-7).

References

Barton N 2007. Rock quality, seismic velocity, attenuation and anisotropy. CRC press.

Giambelluca TW, Chen Q, Frazier AG, Price JP, Chen YL, Chu PS, Eischeid J, Delparte DM 2013. Online rainfall atlas of Hawai'i. Bulletin of the American Meteorological Society 94(3); 313-316.

Goodfellow BW, Chadwick OA, Hilley GE 2014. Depth and character of rock weathering across a basaltic-hosted climosequence on Hawai ‘i.. Earth Surface Processes and Landforms 39(3); 381-398.

Harp E, Hartzell SH, Jibson RW, Ramirez-Gusman L 2012. Relation of landslides triggered by the Kiholo Bay earthquake and modeled ground motion. Landslides and Engineered Slopes: Protecting society through Improved Understanding – Eberhardt et al., (eds), London.

Hayashi K, Suzuki H 2004. CMP cross-correlation analysis of multichannel surface wave data. Exploration Geophysics 35; 7-13.

Hayashi K, Takahashi T 2001. High resolution seismic refraction method using surface and borehole data for site characterization of rocks. International Journal of Rock Mechanics and Mining Sciences 38(6); 807-813.

Lamb MP, Howard AD, Dietrich WE, Perron JT 2007. Formation of amphitheater headed valleys by waterfall erosion after large-scale slumping on Hawai ‘i. Geological Society of America Bulletin 119(7-8); 805-822.

OYO Corporation (2006). SeisImager/2D manual, Ver. 3.2. Available at ftp://geom.geometrics.com/pub/seismic/SeisImager/Intallation_CD/SeisImager2D_Manual/ (verified 2015)

Park CB, Miller RD, Xia, J 1998. Imaging dispersion curves of surface waves on multi channel record. Expanded Abstracts: 68th Annual International Meeting, Society of Exploration Geophysicists 1377-1380.

Stokoe KH, Santamarina JC 2000. Seismic-wave-based testing in geotechnical engineering. ISRM International Symposium. International Society for Rock Mechanics.

Von Voigtlander J 2016. P-wave velocity of weathering profiles from a basalt climosequence: Implications for weathering on the mechanical properties of the critical zone, University of Michigan, M.S. Thesis.

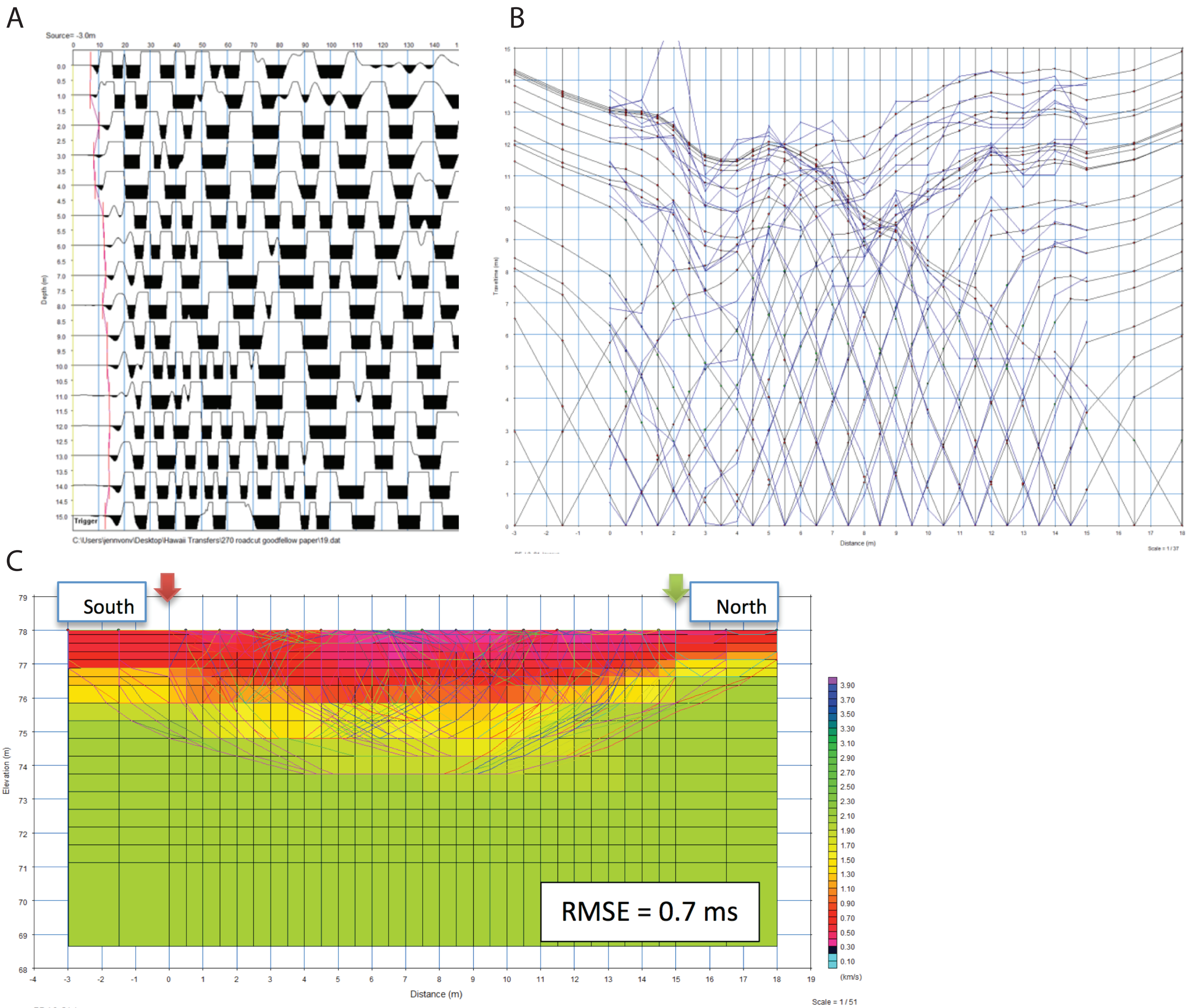

Supplementary Figure 1. Example data from dry sites (Road Cut Site Line 2). A) Wave form data with first break pick assignments (red). Pink line represents the travel time curve. B) Observed versus theoretical travel time curves. C) Linearized model after 60 iterations with ray path coverage shown. Geophone array noted by arrows.

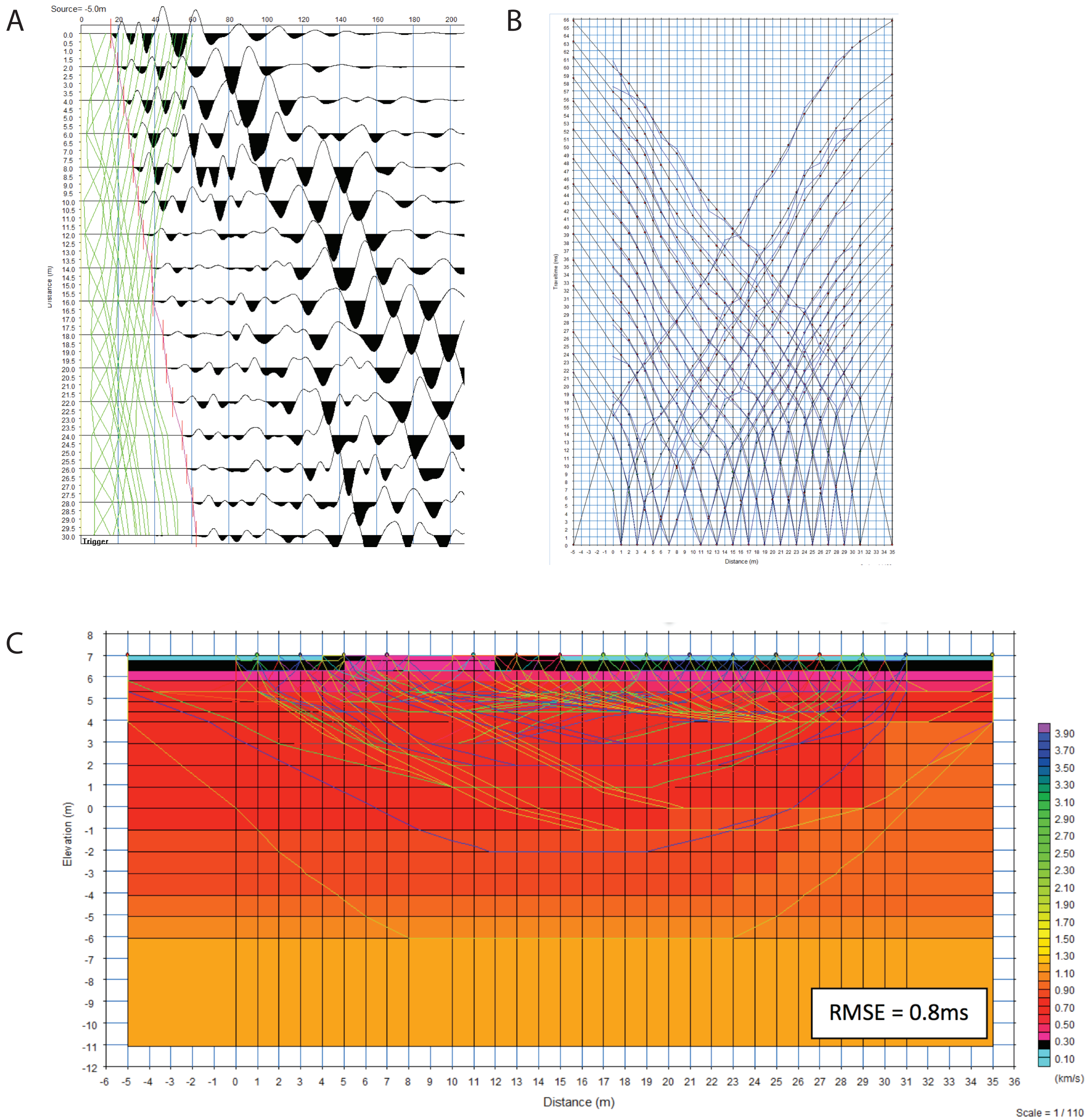

Supplementary Figure 2. Example data from wet sites (Lighthouse line 2). A) Wave form data with first break pick assignments (red). Pink line represents the travel time curve. B) Observed (blue) versus calculated (black) travel time curves from the linearized model. C) Linearized model with ray path coverage shown.

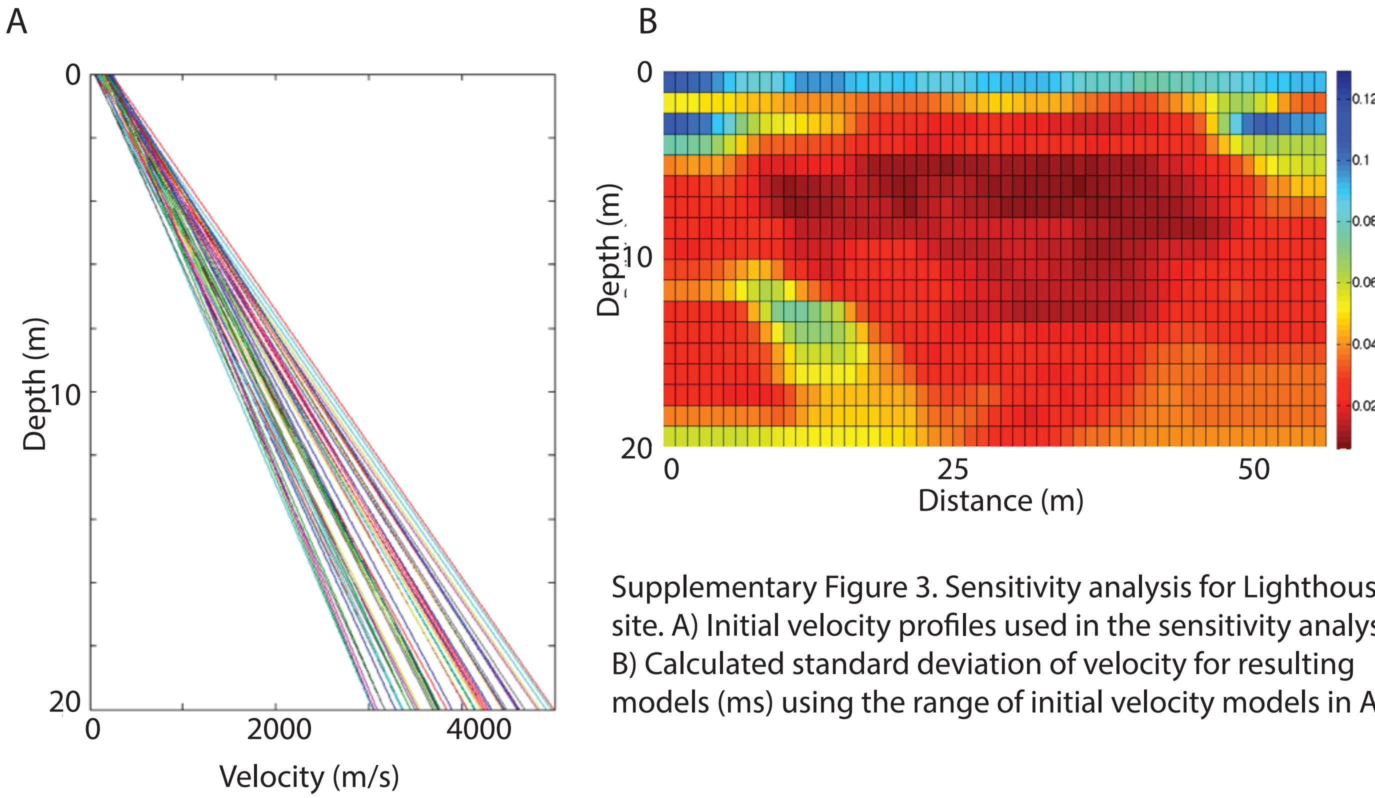

Supplementary Figure 3. Sensitivity analysis for Lighthouse site. A) Initial velocity profiles used in the sensitivity analysis. B) Calculated standard deviation of velocity for resulting models (ms) using the range of initial velocity models in A.

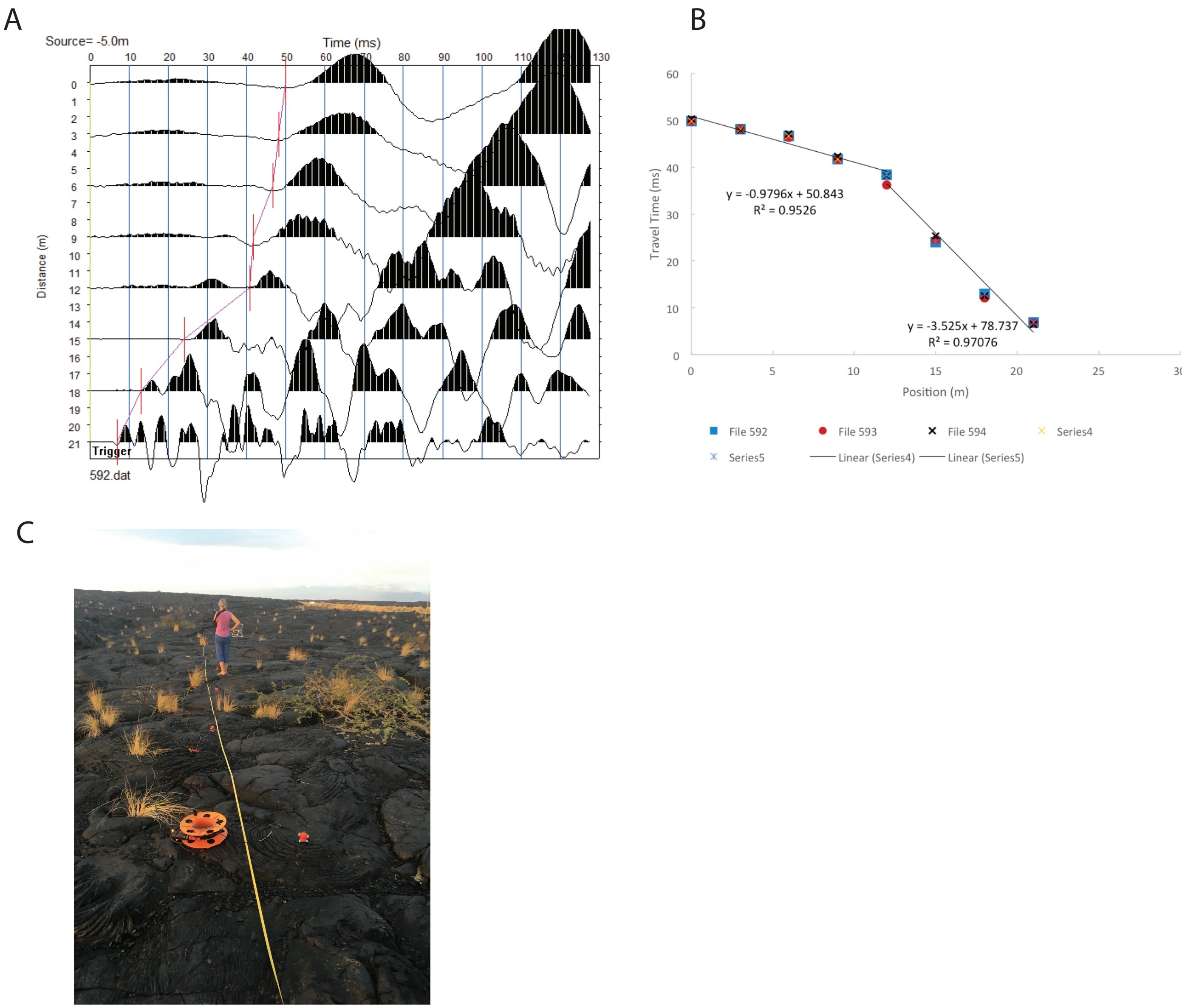

Supplementary Figure 4. 1D Vp profiles from historic flow (1859 A.D.) near Kiholo Bay, Hawaii. A) Example waveform data and first-break picks (red). Pink line denotes travel-time curve. B) Travel time curve for three repeat trials. Near surface velocity is equal to the inverse slope of linear time-distance segments and ranges from ~ 300 - 1000 m/s. C) Photograph of fresh lava surface at survey site.

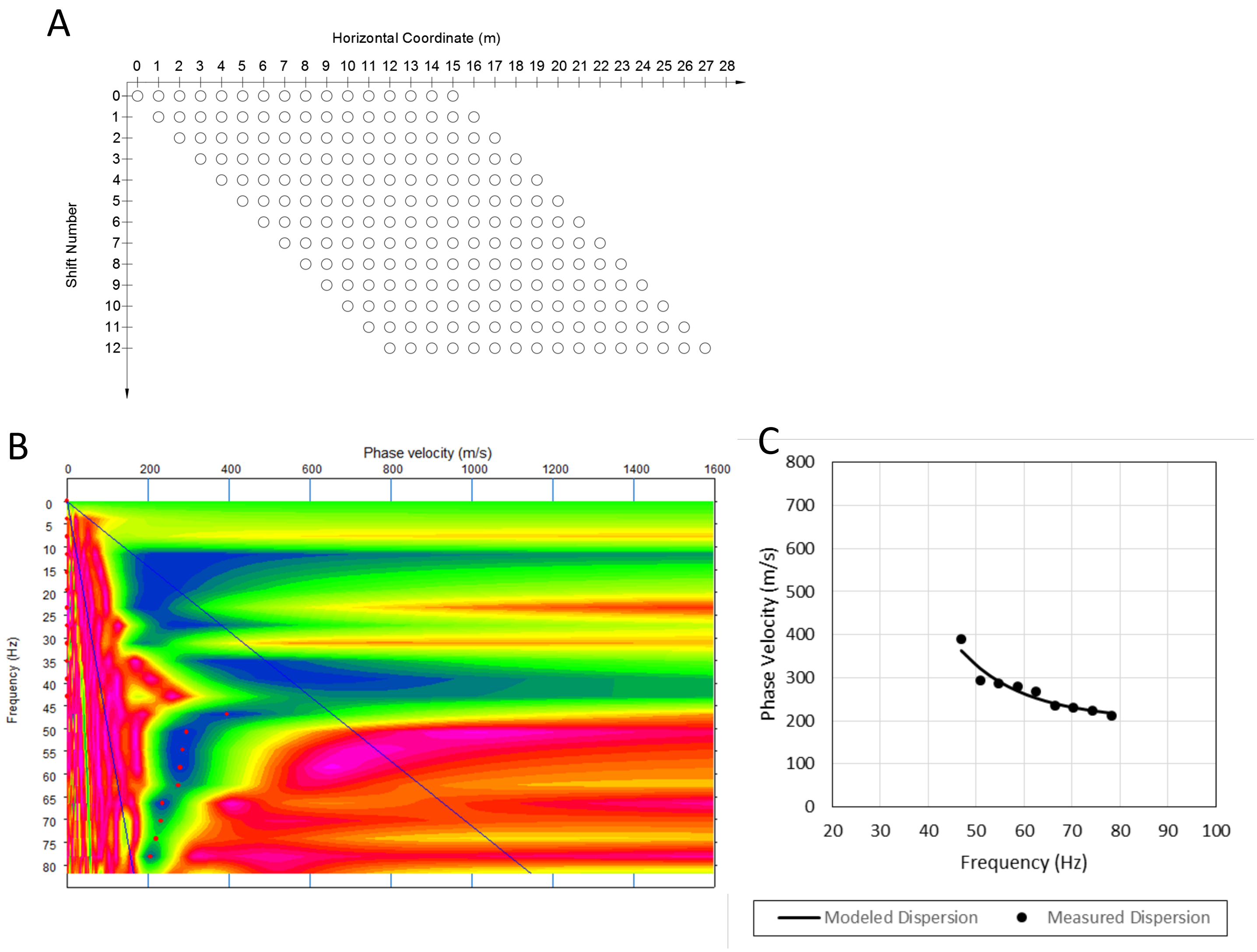

Supplementary Figure 5. MASW survey and data from the Upolo airport site (wet). A) Schematic of 2D MASW testing setup showing location of geophones. Shot and geophone location were shifted by one sensor spacing (1 m) in the direction of the array. Each shifted geometry is shown adjacent to the previous geometry for illustrative purposes. B) Frequency-Phase velocity diagram (blue showing preferred phase velocity for each Rayleigh wave frequency, red points show selected dispersion points plotted in part C. C) Measured dispersion points from B and modeled dispersion curve.

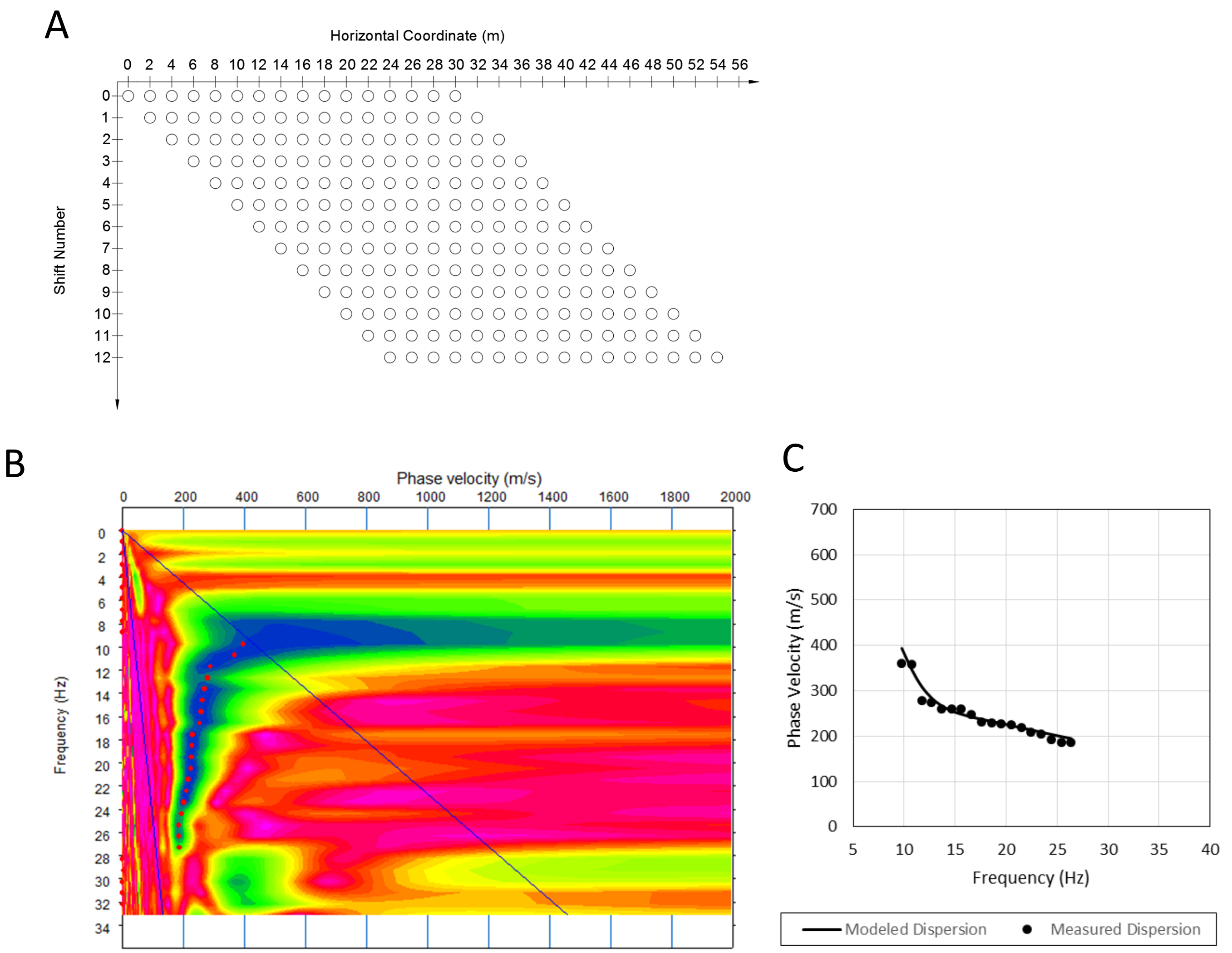

Supplementary Figure 6. MASW survey and data from the Lighthouse airport site (wet). A) Schematic of 2D MASW testing setup showing location of geophones. Shot and geophone location were shifted by one sensor spacing (2 m) in the direction of the array. Each shifted geometry is shown adjacent to the previous geometry for illustrative purposes. B) Frequency-Phase velocity diagram (blue showing preferred phase velocity for each Rayleigh wave frequency, red points show selected dispersion points plotted in part C. C) Measured dispersion points from B and modeled dispersion curve.

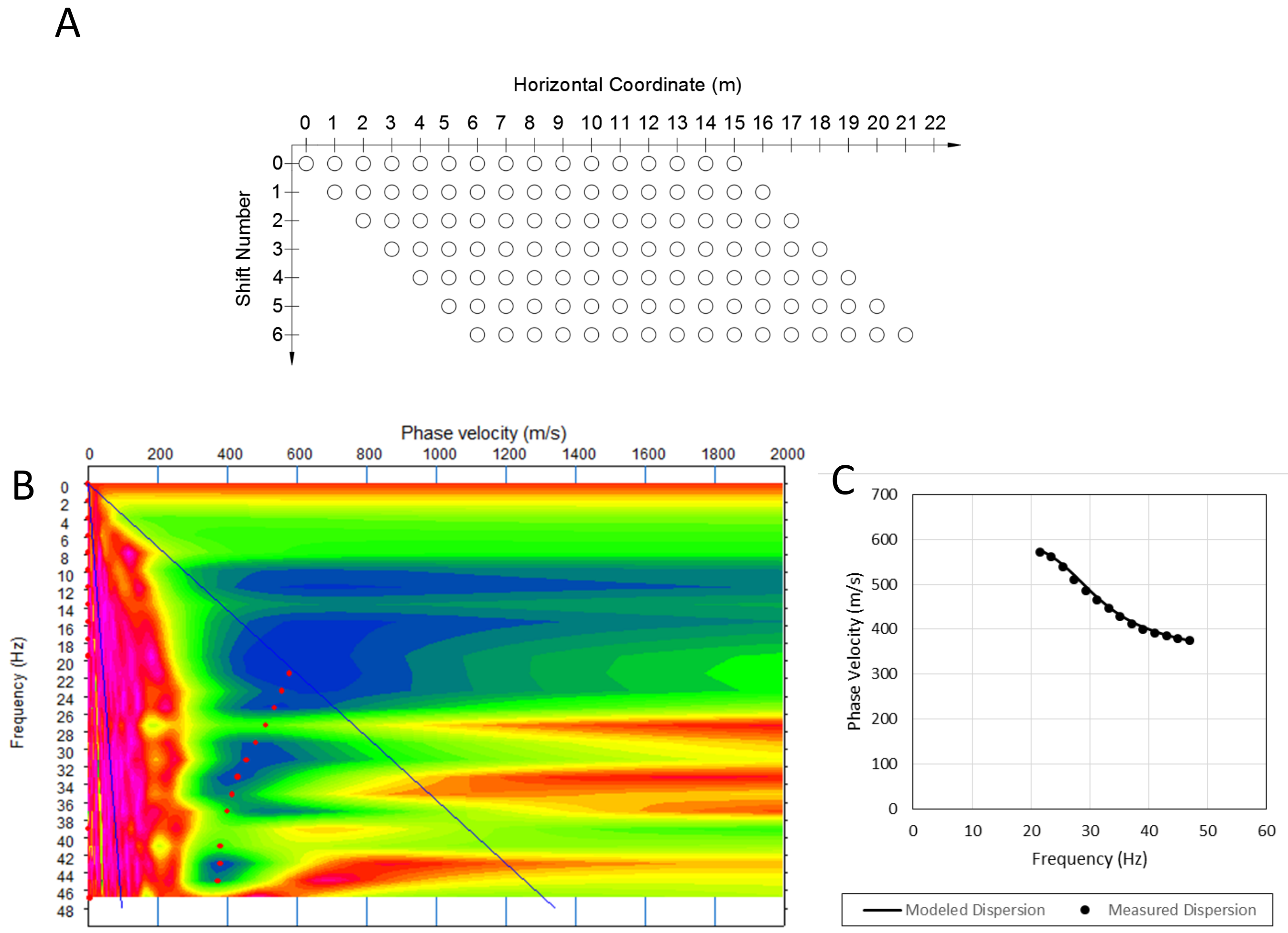

Supplementary Figure 7. MASW survey and data from the Highway 270 road cut east site (dry). A) Schematic of 2D MASW testing setup showing location of geophones. Shot and geophone location were shifted by one sensor spacing (1 m) in the direction of the array. Each shifted geometry is shown adjacent to the previous geometry for illustrative purposes. B) Frequency-Phase velocity diagram (blue showing preferred phase velocity for each Rayleigh wave frequency, red points show selected dispersion points plotted in part C. C) Measured dispersion points from B and modeled dispersion curve.

Supplementary Table 1: Seismic survey sites

Site Name	*Latitude (degrees)*	*Longitude (degrees)*	*Elevation (m)*	*Mean Annual Precipitation (mm)*
Highway 270 Roadcut East	20.1361 N	155.88607 W	78 m	500 mm
Highway 270 Roadcut West	20.13669 N	155.88645 W	78 m	500 mm
Sapphire Cove	20.16220 N	155.89844 W	8 m	500 mm
Kapa'a Beach	20.202116 N	155.902483 W	2 m	604 mm
Upolo Airport	20.26493 N	155.86737 W	8 m	1000 mm
Lighthouse	20.24602 N	155.77101 W	7m	1510 mm
Awini Landslide	20.19369 N	155.72258 W	111 m	2070 mm
Waipio Canyon	20.06458 N	155.66764 W	1169 m	3060 mm

Supplementary Table 2: P wave seismic survey and model parameters

Site Name	*Line Number*	*Geophone Spacing (m)*	*Off-end Shot Distance (m)*	*Length of Survey (m)*	*Shot Density*	*Maximum Resolution (m)*	*Depth Surveyed (m)*	*Geophone Frequency (Hz)*	*Geophone Base*	*Hammer Weight(s) (lb)§*	*Model RMSE (ms)*
Highway 270 Roadcut East	1	3 m	5 m	55 m	13	1x1.5m	18 m	4.5 Hz	Tripod	16	1.4
	2	1 m	3 m	21 m	19	0.25x0.5	3 m	4.5 Hz	Tripod	4, 8§	0.7
Highway 270 Roadcut West	1 (start)**	3 m	10 m	65 m	19	0.5x1.0	21 m	40 Hz	Spike	16	1.5
	2 (shift)**	3 m	10 m	65 m	19	0.5x1.0	21 m	40 Hz	Spike	16	1.4
Sapphire Cove	1*	1 m	3 m	21 m	18	0.25x0.5	3 m	4.5 Hz	Spike	16	1.2
	2*	2.5 m	5 m	47.5 m	13	1x1	12 m	4.5 Hz	Spike	8	1.2
Kapa'a Beach	1	1.5 m	3 m	28.5 m	17	0.3x1	5.5 m	4.5 Hz	Spike	8	0.8
Upolo Airport	1 (start)**	3 m	5 m	55 m	13	0.5x1.5	18 m	4.5 Hz	Spike	8	0.9
	2 (shift)**	3 m	5 m	55 m	13	0.5x1.5	18 m	4.5 Hz	Spike	8	1
	3	1 m	3 m	21 m	20	0.25x0.5	7 m	4.5 Hz	Spike	4, 8§	0.5
Lighthouse	1 (start)**	2 m	5 m	40 m	17	0.5x1.0	12 m	40 Hz	Spike	16	0.9
	2 (shift)**	2 m	5 m	40 m	18	0.5x1.0	13 m	40 Hz	Spike	16	0.8
	3	3 m	5 m	55 m	14	1x1.5	18 m	4.5 Hz	Spike	16	1.6
Awini Landslide	1	1 m	2.5 m	20 m	8	0.2x1	4 m	4.5 Hz	Spike	16	0.5
Waipio Canyon	1	3 m	1.5 m	47.5 m	11	1.0x1.5	15 m	4.5 Hz	Tripod	16	4.1

* Lines perpendicular to each other with no overlap

**(start) lines were (shift)ed, first six geophones replaced last six geophones of previous array. 37.5% overlap

§When multiple hammer weights are used, the larger hammer is used for off-end shots only

Supplementary Table 3: S wave seismic survey parameters

Site Name	*Geophone Spacing (m)*	*Off-end Shot Distance (m)*	*Length of Survey (m)*	*Max model depth*	*Number of Array Shifts*	*Geophone Base*	*Hammer Weight (lb)*	*Number of Stacks*	*Recording length (s)*
Highway 270 Roadcut East	1 m	3 m	21 m	13 m	6	Tripod	8	8	0.5
Upolu Airport	1 m	3 m	27 m	13 m	12	Spike	8	8	0.25
Lighthouse	2 m	5 m	54 m	24 m	12	Spike	16	10	1